

A First-Principles Study of the Ag/ α -Al₂O₃(0001) Interface

Yu.F. Zhukovskii^{1,2*}, E.A. Kotomin^{1,3}, B. Herschend², K. Hermansson² and P.W.M. Jacobs⁴

¹Institute of Solid State Physics, University of Latvia, Kengaraga 8, LV-1063 Riga, Latvia

²Materials Chemistry, The Ångström Laboratory, Uppsala University, Box 538, S-751 21 Uppsala, Sweden

³Max-Planck-Institut für Festkörperforschung, Heisenbergstraße 1, D-70569 Stuttgart, Germany

⁴Department of Chemistry, University of Western Ontario, N6A 5B7 London, Canada

Tel.: +371 718 7480, Fax: +371 711 2583, E-mail: quantzh@latnet.lv

URL: <http://www.tiger.cfi.lu.lv/teor/zhuk.html>

*Author to whom correspondence should be addressed.

Received: 25 September 2001 / Accepted: 19 October 2001 / Published: 13 November 2001

Abstract: *Ab initio* simulations of the Ag/ α -Al₂O₃(0001) interface have been performed for periodic slab models. We have considered Al- and O-terminated corundum surfaces, low and high substrate coverages by silver, as well as the two preferred Ag adsorption sites. The two different terminations give rise to qualitatively different results: silver *physisorption* on the Al-terminated substrate and *chemisorption* on O-terminated one. The latter could be treated as a possible model for the defective Al-terminated substrate, where the outermost aluminium ions are removed (completely or partly). This makes O-terminated surface highly reactive towards a deposited metal, in order to restore initial corundum stoichiometry.

Keywords: metal/oxide interface, Ag adsorption, α -Al₂O₃ (corundum), Al- and O-terminated (0001) surfaces, *ab initio*, Hartree-Fock method, electron correlation corrections

1. Introduction

Well-known in jewelry as sapphire, α -Al₂O₃ (*corundum*) nowadays is one of the most widespread ceramic materials [1]. It is used in particular, as an advanced substrate for ultrathin metal film deposition [2]. Alumina-supported transition metal catalysts are of continually growing interest due to their high efficiency in several technologically important reactions including oxidation of CO and hydrogenolysis [3]. In addition to the widespread use of γ -Al₂O₃ as a substrate both stoichiometric and reduced α -Al₂O₃ are also used for this purpose [4]. Moreover, metallic species supported on a corundum substrate, in particular Pd/ α -Al₂O₃ [5], are used quite effectively as model catalysts.

It is generally believed that the Al-terminated surface is energetically favored over the O-terminated one, since the former is stoichiometric and closer to the bulk structure [6]. Nevertheless, the O-terminated corundum surface has been observed experimentally as well [7]. Theoretical studies [8,9] indicate that even under conditions of high oxygen gas partial pressure the Al-terminated corundum surface is stable (contrary to conclusions of the review paper [10]), while even a small hydrogen concentration on the α -Al₂O₃(0001) substrate stabilizes considerably the alternative O-terminated surface. The lower stability of the O-terminated substrate as compared to the Al-terminated one, as well as the presence of O-termination on the defective α -Al₂O₃(0001) surface (containing either steps or flat areas in the vicinity of vacancies in the outermost layer of the Al³⁺ sublattice [11]) could be responsible for some conflicting results [9,10]. The presence of hydrogen on this substrate and its further hydroxylation could also help to explain the discrepancies between some theoretical estimates [12-15] and experimental measurements [8-10] concerning the relaxation of the surface and subsurface crystalline layers of pure corundum.

In our previous investigation of Ag adsorption sites on α -Al₂O₃(0001) [16], using the periodic Hartree-Fock method with *a posteriori* electron correlation corrections (hereafter *HF-CC method*), we found *two* favorable adsorption sites for 1/3 ML silver coverage of the O-terminated α -Al₂O₃(0001) substrate (one Ag atom per three O²⁻ outermost ions, as shown in Figs. 1 and 2a) optimized earlier by Puchin *et al.* [13]. These are:

- (i) Over large equilateral oxygen triangles, where Ag atoms replace surface Al³⁺ ions on an Al-terminated surface; hereafter we call these sites *E2* (closest positions to equilateral surface oxygen triangles shown in Fig. 2a) in contrast to more remote sites *E1* (in Fig. 2b),
- (ii) Over non-equilateral surface oxygen triangles, which lie atop the oxygen ions of the *next* subsurface oxygen layer; we call these sites *H* (hollow), because there are no Al³⁺ ions below these triangles.

Adhesion energies per Ag atom for both sites on the O-terminated surface were estimated to be about 3 eV [16], so that such adhesion cannot be considered as physisorption, the more so because the adsorbed silver atoms become ionized into Ag⁺ ions. Other possible adsorption sites, including Ag positions on top of the outermost O²⁻ ions, were found to be energetically less favorable.

Verdozzi *et al.* [17] have modeled Ag and Pt adhesion to an Al-terminated corundum slab which included 18 oxygen (0001) planes, using Density Functional Theory (DFT) calculations with plane-wave pseudopotentials. Their general conclusion was that the interaction between silver atoms and substrate in the Ag/corundum interface is physisorption, although well-separated metal atoms (1/3 ML) may be more strongly bound due to the effect of the surface Madelung potential. However, they neglected metal adhesion on an O-terminated surface. Similar DFT plane-wave studies were performed for Nb adhesion [18] as well as for Al and Cu adhesion [19] on both the Al- and O-terminated surfaces of a corundum (0001) substrate. It was found that niobium bonding on the O-terminated surface (13 eV per Nb atom) is much stronger than that on the Al-terminated surface (3.4 eV) [18]. Experimental observations of very strong niobium-corundum adhesion have also been associated with O-termination [20]. At the same time, unlike noble silver, Nb is a highly reactive metal, so that the outer aluminium ions of the Al-terminated α -Al₂O₃(0001) surface can be substituted by niobium atoms after their adsorption on the corundum substrate. To clarify the nature of noble metal adhesion on corundum (0001) surface, we present in this paper a quantitative analysis of their interfacial bonding.

2. Method and model

As mentioned previously, we used in these calculations the HF-CC method with Gaussian-type basis sets (BSs) as implemented in the computer code CRYSTAL98 [21]. The Perdew-Wang functional (PWGGA [22]) was mainly used in a posteriori electron correlation corrections. To perform better CRYSTAL simulations on corundum, Catti et al. [23] modified the all-electron basis sets used in previous α - Al_2O_3 studies [12,13] by introducing a 3d-polarization function in addition to sp-polarization functions and by re-optimizing core and valence shells. Thus, for aluminium and oxygen ions, we use 8(s)-511(sp)-1(d) and 8(s)-411(sp)-1(d) BSs, respectively [23]. For silver atoms, the same Ag BS was used as earlier [16], employing the small-core Hay-Wadt pseudopotential for the atomic core [24] and 311(sp)-31(d) Gaussian-type functions for both valence and virtual shells. The energies quoted in this paper include the BS superposition errors (BSSE) evaluated according to the standard procedure implemented in CRYSTAL98 [21].

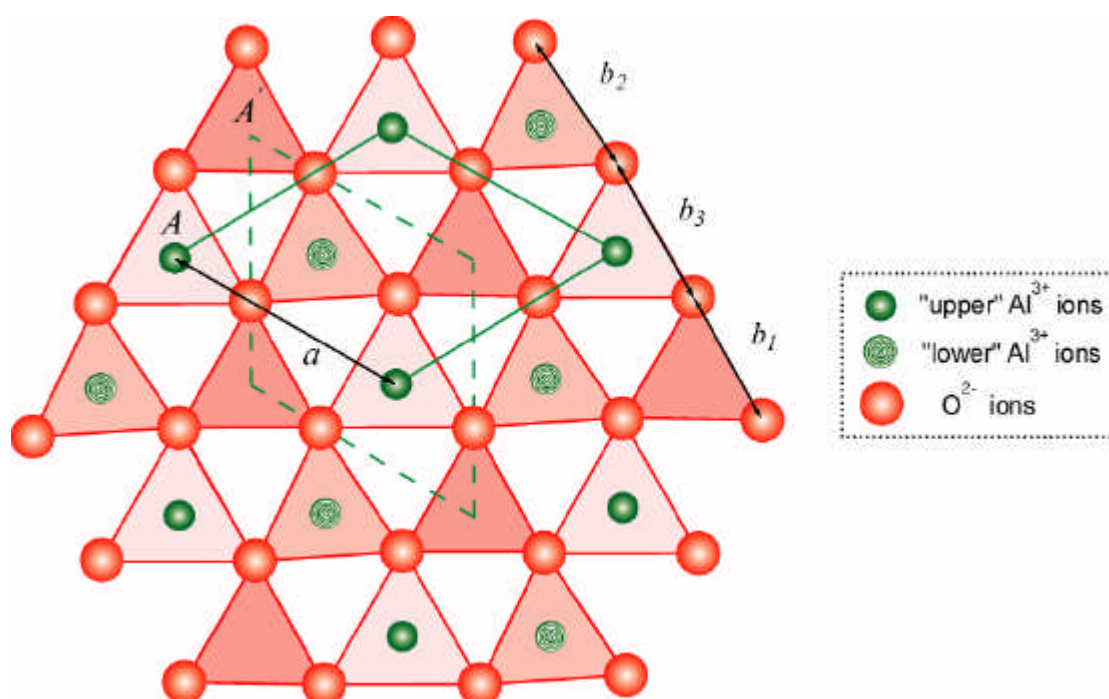


Figure 1. Top view of the oxygen plane of the corundum (0001) substrate, as optimized in [13], and two neighboring aluminium planes positioned above and below the oxygen plane (green circles with different internal patterns). In these planes, Al^{3+} ions form a hexagonal network with a rhombic unit cell, whereas O^{2-} ions form a more complicated regular structure containing equilateral triangles of three different sizes. Each may be distinguished by the shade of red color used, the larger the triangle the lighter the shading used. Intermediate versatile triangles are shown in white.

For the simulation of silver adhesion on the corundum substrate, we have used a *slab model*, periodic in two dimensions, and of finite thickness in the direction perpendicular to the (0001) plane [12]. The α - Al_2O_3 (0001) substrate belongs to the hexagonal plane group P_{321} , the optimized length of the side a in its surface unit cell being 4.76 Å (Fig. 1). Both a 7-layer slab with outermost oxygen ions (Fig. 2a) and a 9-layer slab terminated by aluminium ions (Fig. 2b) have been modeled, using primitive unit cells that contained 13 and 15 atoms, respectively. The C_{3v} rotation axes normal to the surface contain Al^{3+} ions and form a regular network normal to a (111) plane of the face-centered cubic (*fcc*) structure, this plane being parallel to the (0001) plane. The distance $AA' = a/\sqrt{3}$ between adjacent

Al^{3+} axes is 2.75 Å; the two rhombic surface unit cells formed by those axes are shown in Fig. 1. All the O^{2-} ions in the bulk corundum are equivalent; its slab structure optimized by Puchin *et al.* [13] forms a periodic network of *equilateral* triangles with b_1 , b_2 and b_3 sides (2.64 Å, 2.74 Å and 2.87 Å, respectively), as well as *versatile* triangles positioned between them (Fig. 1). The oxygen-containing corundum (0001) planes are equivalent, with an interplanar distance $c \approx 2.16$ Å (Fig. 2). Each oxygen plane can be transformed into a neighboring one by a synchronous combination of a 60° rotation around the corresponding C_{3v} axes and a translation by AA' (Fig. 1), so that the two rhombic surface unit cells (Fig. 1) coincide. Each oxygen plane is associated with two adjacent, less-densely packed aluminium planes, so that each Al^{3+} ion is positioned either above the center of the largest equilateral oxygen triangle or below the middle triangle (at a distance d of 0.84 Å in bulk corundum).

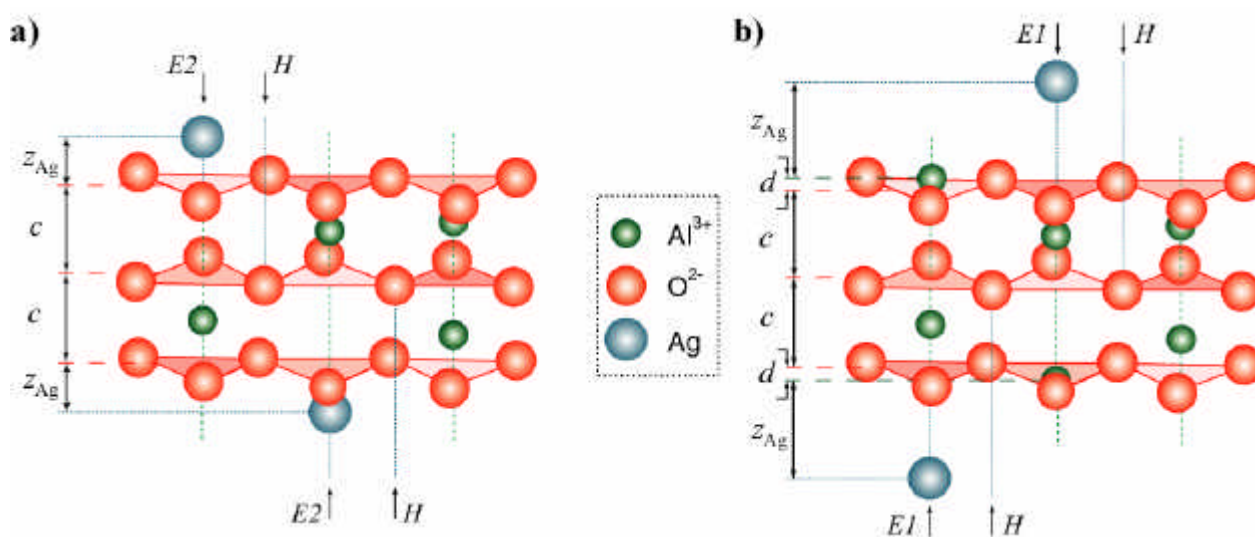


Figure 2. Side views of $\alpha\text{-Al}_2\text{O}_3(0001)$ slabs where silver atoms at 1/3 ML coverage are distributed regularly on the aluminium C_{3v} axes above and below O-terminated (a) and Al-terminated (b) models, respectively. The interlayer structure of the interface is defined by c , d and z_{Ag} parameters. The most probable positions for Ag adsorption have been found to be $E1$ for (b), $E2$ for (a), and H .

In this study, we have varied the interfacial distance z_{Ag} for both terminations (Table 1) and the Al–O plane distance d for the Al-terminated corundum substrate (its optimized value is analyzed in subsection 3A). To reduce computational effort we exploited the system’s symmetry by applying a two-side adhesion model, with spatially equivalent silver layers on *both* surfaces of the corundum slab. For both Al- and O-termination we have considered two different Ag coverages: 1/3 ML (Fig. 3a) and 1 ML (Fig. 3b). For a 1/3 Ag ML coverage of the Al-terminated slab, two different adsorption patterns have been modeled: silver atoms over the smallest equilateral oxygen triangles, site $E1$ (Fig. 2b), or Ag over versatile O triangles, *i.e.* above 1/3 of the H sites (Fig. 3a). For the 1/3 Ag ML coverage of the O-terminated slab, two patterns have been also used: silver atoms above the largest equilateral oxygen triangles, site $E2$ (Fig. 2a), or Ag above 1/3 of the same H sites. In both cases, silver atoms are distributed regularly on the substrate forming a periodic $\sqrt{3} \times \sqrt{3}$ superstructure. For 1 Ag ML coverage, two different adsorption patterns have been also considered for both terminations: either above all equilateral triangles or above all the H sites (Fig. 3b). Space and symmetry compatibility between the Ag(111) and $\alpha\text{-Al}_2\text{O}_3(0001)$ planes mentioned above allows us to consider relatively simple models of the Ag/corundum interface without the inclusion of misfit dislocations.

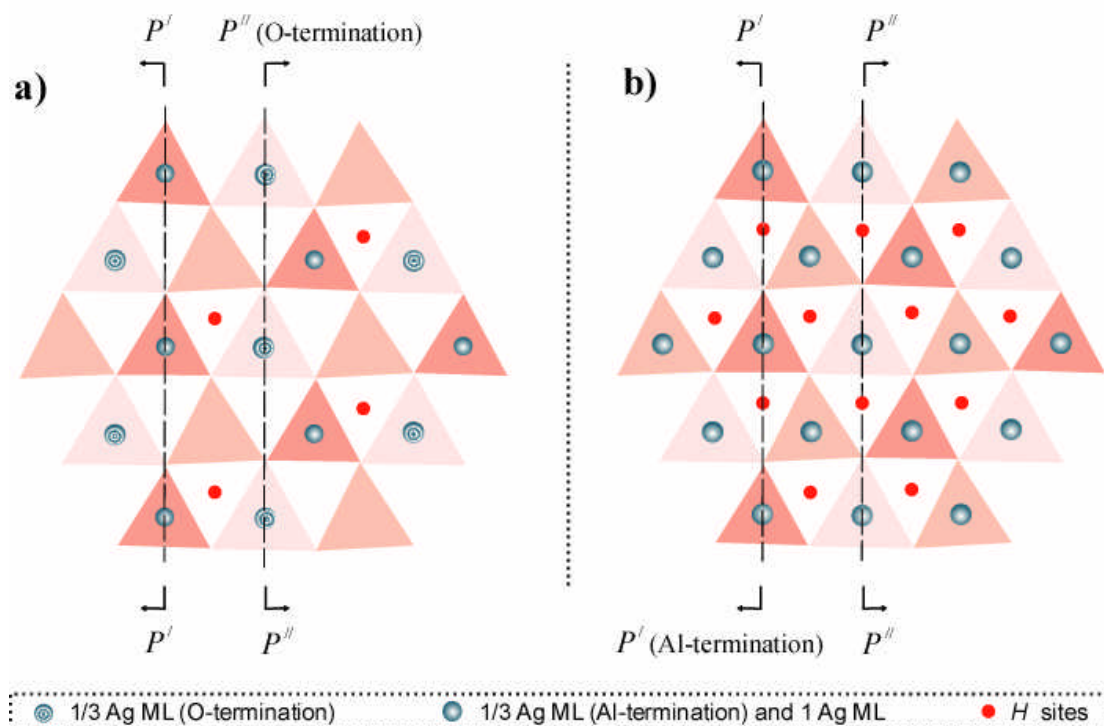


Figure 3. Top views of Ag atom distributions over Al- and O-terminated corundum (0001) surfaces for the two different coverages: 1/3 ML of the Ag(111) plane (a) and 1 Ag ML (b). The two different silver atom adsorption positions are above equilateral and versatile triangles forming the outermost O plane. Circles with two different internal patterns (a) show the two kinds of Ag atom distributions over equilateral triangles on Al- and O-terminated substrates, whereas positions over versatile triangles are shown by red dots in both (a) and (b). Planes P' – P'' and P' – P'' are used in Figs. 4 and 5, respectively, to show the electron charge density distributions in cross sections perpendicular to the (0001) surface.

The binding (adhesion) energy *per* silver atom at the equilibrium distance, E_{bind} (Table 1), is estimated as a straightforward energy difference:

$$E_{bind} = -\frac{E_{Ag/corundum\ slab} - (E_{Ag\ slab} + E_{corundum\ slab})}{k}, \quad (1)$$

where $E_{Ag/corundum\ slab}$ is the total energy for the interface at the equilibrium Ag-corundum slab distance; $E_{Ag\ slab}$ and $E_{corundum\ slab}$ are the total energies for the corresponding isolated subsystems with the *same* geometry as that of the optimized interface system; $k = 2$ for the model with two-side adhesion. The change of the silver Mulliken charge, Dq_{Ag} , characterizes the interfacial electronic charge transfer (Table 1). To obtain a greater insight into the nature of the interaction between the corundum surface and quasi-isolated silver adatoms (1/3 ML) or the full (111) monolayer, we have plotted several 2D sections of the *difference* electron density distribution $D\rho(\mathbf{r})$ across the interface (Figs. 4 and 5). This charge redistribution function is defined as:

$$D\rho(\mathbf{r}) = \rho_{Ag/corundum\ slab}(\mathbf{r}) - [\rho_{Ag\ slab}(\mathbf{r}) + \rho_{corundum\ slab}(\mathbf{r})], \quad (2)$$

i.e. the total electron density $\rho_{Ag/corundum\ slab}(\mathbf{r})$ minus a superposition of the densities for the two isolated metal and corundum slabs, $\rho_{Ag\ slab}(\mathbf{r})$ and $\rho_{corundum\ slab}(\mathbf{r})$, respectively, with the same geometry as they have in the interface system. Each density plot can clearly demonstrate the effects resulting from the interfacial interactions. The projections for the cross-sections used for these plots are defined in Fig. 3.

3. Results and discussion

A. Al-terminated substrate

Our results for the low and high (1/3 ML and 1 ML) substrate coverages show important characteristics concerning the silver-oxide binding (Fig. 4 and Table 1). The equilibrium Al–O interlayer distance d (Fig. 2b) in the Ag/corundum interface (0.12 Å) is almost unchanged from its value in the isolated Al-terminated substrate (0.14 Å) although Verdozzi et al. [17] found significant outward Ag-adsorbate-induced relaxation of the same Al–O interlayer. Silver adhesion over the E1 sites (Fig. 2b) is the most favorable for 1/3 Ag ML coverage, but an H site is found to be an alternative, slightly less stable, position for Ag atom localization on the substrate. Moreover, there are certain structural restrictions on Ag atoms over hollow sites, which result in a tendency to form monolayers and thicker overlayers (Fig. 3b). While a periodic network formed by the centers of all equilateral oxygen triangles (normal to axes containing Al³⁺ ions) corresponds completely to the symmetry of the Ag(111) plane (Fig. 3b), the alternative network over H sites, which repeats the distribution of O²⁻ ions in the subsurface oxygen plane, may be treated as a *distorted* Ag(111) surface. Such a monolayer film is not very stable in an isolated state and its further growth is rather problematic. The regular Ag(111) monolayer in profile, is found to be buckled because silver atoms on the corundum substrate tend to preserve the same interatomic distance as in bulk silver (the experimental value of $a_{\text{Ag-Ag}}^{(\text{min})} \approx 2.88$ Å [25] exceeds the distance of 2.75 Å between the neighboring Al³⁺ axes). The height of steps in the buckled silver monolayer (h_{Ag}) was optimized to be 0.7 Å (the “external” Ag rows, the most remote from substrate, lie atop external Al³⁺ ions, whereas the “internal” Ag rows, the closest to surface, lie over the second internal sublayer of Al³⁺ ions as shown in Fig. 2b). Since the “internal” Ag atoms are slightly positively charged (+0.1 e), they are attracted to the equilateral triangles formed by outermost O²⁻ ions. The ratio of the binding energies *per* Ag atom for 1/3 and 1 ML adsorption over equilateral oxygen triangles is two: 0.54 eV versus 0.27 eV (Table 1). The corresponding data obtained by Verdozzi et al. [17] agree qualitatively with our results but with a ratio of three: 1.1 eV versus 0.36 eV. (Such quantitative discrepancies may be due to the fact that the HF method underestimates binding energies, whereas DFT calculations sometimes overestimate them [26].) This probably occurs because each Ag atom in the 1/3 ML may interact directly with *three* nearest O²⁻ ions, while for 1 Ag ML, the number of silver atoms equals that of oxygen ions. For 1/3 Ag ML, the electron density redistribution is found to be mainly localized around both silver atoms and Ag–O bonds (Fig. 4a). However, the interatomic electron density in a silver monolayer is enhanced as compared to pure Ag film (Fig. 4b), showing that adsorbed silver atoms are still connected by metallic bonds and interact less favorably with the oxygen triangles below, thus reducing the interfacial bonding per Ag atom. For both coverages, a lower electron density in the interfacial area (colored in blue) is probably caused by the screening influence of the outer Al³⁺ ions. As in our previous simulations on the perfect Ag/MgO (100) and (110) interfaces [27], the small values of adhesion energy per Ag atom ($E_{\text{bind}} < 1$ eV) and negligible charge transfer across the interface between Ag adsorbate and Al-terminated corundum (Table 1) indicate that the nature of silver adhesion is *physisorption*. In all three cases mentioned above, the interfacial charge redistribution is mainly limited to electronic charge polarization in the rather close vicinity of the Ag nuclei. Moreover, the internal ions of corundum slab are practically not involved in the interfacial bonding (Fig. 4).

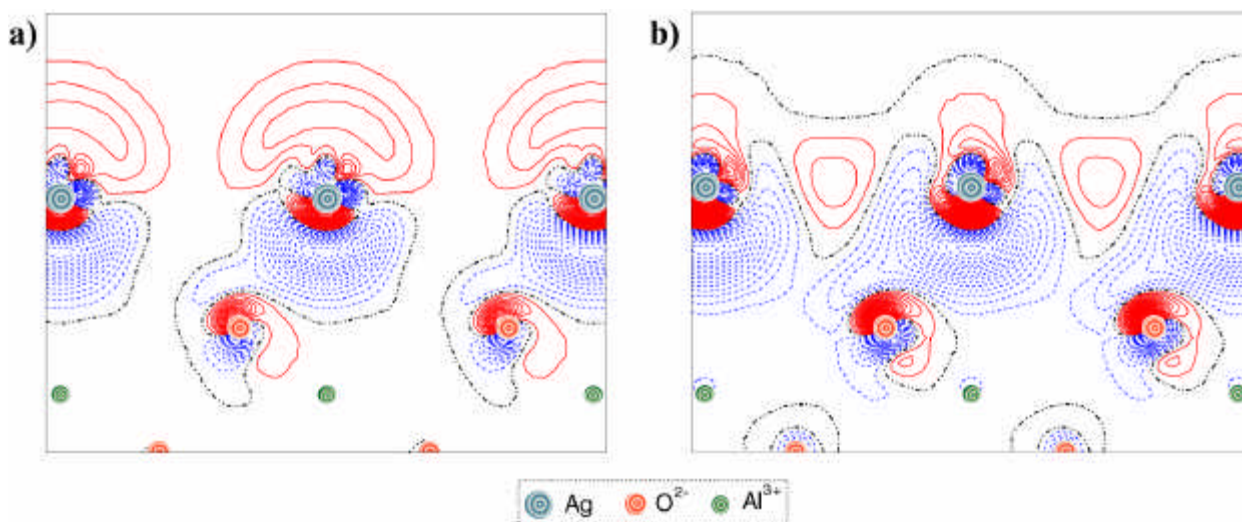


Figure 4. Cross-sections of difference electron density distributions $D\mathbf{r}(\mathbf{r})$ defined by Eq. (2) for two different coverages in the case of E configurations of silver atoms adsorbed on the Al-terminated substrate: (a) 1/3 Ag ML (Fig. 2b) and (b) 1 Ag ML. In order to mark in the centers of atoms and ions lying in the cross-sections shown in Fig. 3, colored circles with the three different patterns are used. Bottom borderlines of plots correspond to a central oxygen plane shown in Fig. 2b. Isodensity contours are drawn from $-0.3 e \text{ au}^{-3}$ to $+0.3 e \text{ au}^{-3}$ with an increment of $0.0004 e \text{ au}^{-3}$. The full (red), dashed (blue) and chained (black) curves show positive, negative and zero difference densities, respectively.

Table 1. Optimized parameters for different slab models of the Ag/ α -Al₂O₃(0001) interface. Silver atom positions over both equilateral and versatile oxygen triangles for different substrate terminations and coverages are shown in Fig. 3.

Ag adhesion over the centers of:	Substrate coverage by Ag(111)	Distance $z_{\text{Ag}}^{\text{a)}$, Å	Binding energy E_{bind} , eV	Mulliken charge $Dq_{\text{Ag}}^{\text{b)}$, e
<i>Al-terminated corundum substrate</i>				
equilateral O triangles	1/3 ML	2.21	0.54	+0.01
	1 ML	2.49	0.27	(A) ^{c)} +0.11
				(B) ^{c)} +0.04
(C) ^{c)} -0.15				
versatile O triangles	1/3 ML	2.39	0.40	+0.01
	1 ML	2.77	0.12	-0.01
<i>O-terminated corundum substrate</i>				
equilateral O triangles	1/3 ML	1.12	10.5	+0.89
	1 ML	1.23	5.0	(A) ^{c)} +0.42
				(B) ^{c)} +0.40
(C) ^{c)} +0.32				
versatile O triangles	1/3 ML	1.32	11.6	+0.64
	1 ML	1.56	4.7	+0.42

^{a)} Optimized distance between Ag atom closest to a surface and an outer substrate layer (Fig. 2).

^{b)} Negative and positive values of Dq_{Ag} mean excess and deficiency of electronic charge, respectively, as compared to neutral Ag atom.

^{c)} Charge transfer on a stepped Ag(111) layer calculated for “internal” (A), “middle” (B), and “external” (C) silver atoms, see description in the text.

B. O-terminated substrate

The 1/3 Ag ML coverage may be considered as a result of the substitution of all aluminium ions on a stable Al-terminated corundum (0001) surface by silver atoms (Fig. 2a). This is associated with a large binding energy. Since an isolated O-terminated corundum (0001) substrate is non-stoichiometric, the presence of a metal film strongly stabilizes the surface. The charges of the oxygen ions in the outermost plane of the isolated substrate turn out to be closer to O^- than O^{2-} , which facilitates charge transfer from metal to substrate. Moreover, as Table 1 shows, in a 1/3 Ag ML, an adsorbed silver atom is closer to an Ag^+ ion than to an Ag atom. Unlike the inward relaxation of the top Al corundum layer, the Ag layer relaxes *outwards* by up to 20-25% of the equilibrium Al–O distance d in bulk corundum (Fig. 2a). For 1/3 Ag ML, the most stable adsorption position is found to be the *H* site above versatile O triangles (Fig. 3a), with a binding energy per Ag^+ ion about 11.6 eV. *E2* sites above the large equilateral oxygen triangles (Fig. 2a) were found to be slightly less favorable. This is probably due to the additional electrostatic interaction of Ag^+ ions with the O^{2-} ions of the next subsurface oxygen plane. On the Al-terminated corundum surface, influence of the latter is considerably reduced by the outer aluminium ions. The much larger value of binding energies E_{bind} , as compared to a silver adsorption on the Al-terminated surface (Table 1), accompanied by a significant charge transfer to the substrate, clearly indicates chemisorption. Our values for E_{bind} for 1/3 Ag ML on the O-terminated corundum (0001) surface agree qualitatively with the corresponding results of Batyrev et al. [18,19] for Al, Cu and Nb adhesion on the same substrate (11.3 eV, 7.5 eV and 13.0 eV per adsorbed metal atom, respectively).

Comparison of the two difference electron density distributions, shown in Figs. 4a and 5a, confirms our conclusions about the nature of interfacial bonding. The outermost oxygen ions of an Al-terminated substrate experience rather weak charge distortion compared to adsorbed silver atoms. In the case of O-termination, external oxygen ions are strongly involved in chemical Ag–O bonding, moreover, internal O^{2-} ions participate in this bonding as well (unlike the charge redistribution shown in Fig. 4a).

For 1 Ag ML coverage on the O-terminated surface, we find some qualitatively common features with the Al-terminated interfaces, except for the nature of the interfacial bonding. Again, a buckled Ag(111) monolayer positioned above the centers of all the equilateral oxygen triangles (Fig. 3b) is energetically more favorable than a monolayer over the hollow-site triangles. The optimized value of the silver step height in this case ($h_{Ag} \approx 0.4 \text{ \AA}$) is smaller than that for the Al-terminated substrate. The ratio of the binding energies per Ag atom for the 1/3 ML and 1 ML cases for the buckled silver monolayer (≈ 2.1), is rather similar to that for Al-terminated corundum. The dependence of E_{bind} on coverage can be also explained analogously, by a change of Ag coordination numbers: for the lower coverage, the silver ion interacting more strongly with the nearest oxygen ions than that in the case of monolayer coverage. This also explains the larger charge transfer per Ag^+ ion in the former case (Table 1). Moreover, when comparing Figs. 4b and 5b one can observe a noticeable difference in the interfacial bonding of a silver monolayer with Al- and O-terminated corundum substrates. Unlike the former case discussed in subsection 3A, the interatomic electron density in the silver monolayer positioned over external oxygen ions is reduced as compared to pure Ag film. This confirms that interaction along the interface Ag–O bonds is so strong that the metallic properties of a silver film practically disappear.

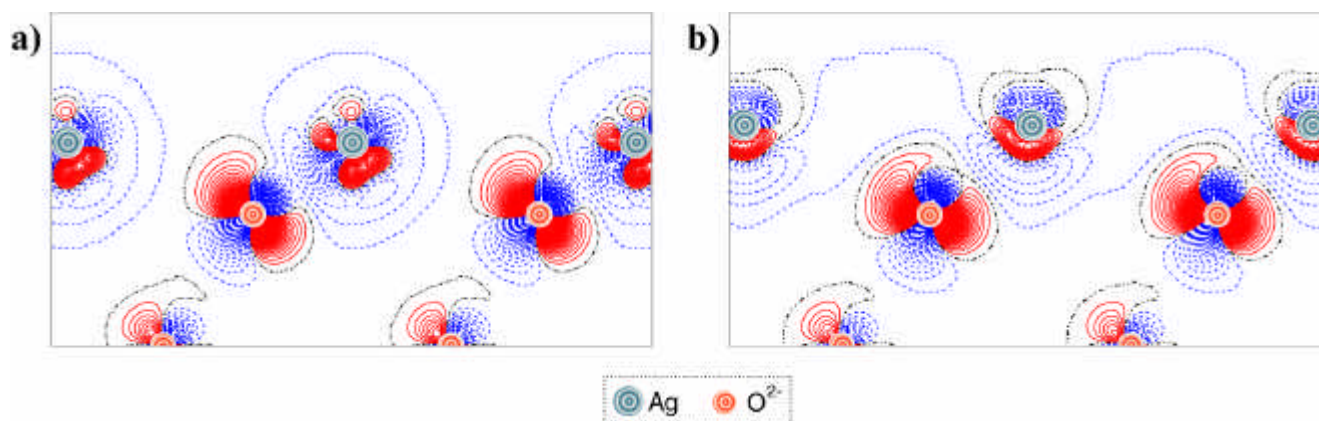


Figure 5. The pair of electron density plots similar to those shown in Fig. 4, but for O-terminated substrate (Figs. 2a and 3): 1/3 Ag ML (a) and 1 Ag ML (b). Note that the isodensity curves are drawn from $-0.3 e \text{ au}^{-3}$ to $+0.3 e \text{ au}^{-3}$, with 10 times larger increments ($0.004 e \text{ au}^{-3}$) than those used for Al-terminated substrate. Thus, density plots shown in Figs. 4 and 5 can only be compared qualitatively.

The strong chemisorption of Ag on the O-terminated corundum surface can be seen as a consequence of metal adsorption on a *defective* Al-terminated substrate, where the outermost Al^{3+} ions are removed and thus silver atoms are adsorbed on *aluminium vacancies*. Indeed, as observed in a study of Ag adsorption on both a perfect $\text{MgO}(100)$ surface and one with Mg^{2+} vacancies [28], the vacancies are filled by positively charged silver ions, and the adsorption energy increased by more than an order of magnitude compared to the perfect oxide substrate.

4. Summary

We have shown that silver adhesion on Al- and O-terminated corundum substrates differ qualitatively, both in the binding energies and charge transfer across the interface. For Al-termination, which corresponds to an equilibrium state of the corundum substrate, we observe much smaller adhesion energies per Ag atom and negligible interfacial charge transfer, which clearly indicate *physisorption*. In contrast, for the O-terminated corundum, a substantial binding energy per Ag atom is combined with noticeable charge transfer (up to $0.9 e$) towards the corundum substrate, indicating *chemisorption*. Since the strength and nature of metal-support interaction is always a highly relevant question in catalytic contexts, we consider our results from this point of view as well. The outer aluminium ions on the Al-terminated substrate surface screen the favorable interaction between the silver atoms and the outermost oxygen triangles. Thus from our calculations one might suspect that the Al-terminated alumina support makes Ag more prone to be catalytically active than does the O-terminated support.

Acknowledgements.

This study was supported by the EC Excellence Centre of Advanced Material Research and Technology (Contract Nr ICA1-CT-2080-7007) in Riga, Latvia, and a STINT Institutional grant Nr 99/899 promoting Swedish-Canadian scientific collaboration. The authors thank O. Sychev for assistance with preparation of the figures.

References and Notes

1. Gitzen, W. H. *Alumina as a Ceramic Material*; Publ. Amer. Ceram. Soc.: Columbus (OH), 1970.
2. Campbell, C. T. *Surf. Sci. Reports* **1997**, *27*, 3.
3. Henry, C. R. *Surf. Sci. Reports* **1998**, *31*, 235.
4. Stara, I.; Nehasil, V.; Matolin, V. *Surf. Sci.* **1996**, *365*, 69.
5. Ladas, S.; Poppa H.; Boudart, M. *Surf. Sci.* **1981**, *102*, 151.
6. Guo, J.; Ellis, D. E.; Lam, D. J. *Phys. Rev. B* **1992**, *45*, 3204.
7. Bruley, J.; Brydson R.; Müllejans, H.; Mayer, J.; Gutekunst, G.; Mader, W.; Knauss, D.; Rühle, M. *J. Mater. Res.* **1994**, *9*, 2574.
8. Tepesch, P. D.; Quong A. A. *Phys. Stat. Solidi (b)* **2000**, *217*, 377.
9. Wang, X. G.; Chaka, A.; Scheffler, M. *Phys. Rev. Letters* **2000**, *84*, 3650.
10. Renaud, G. *Surf. Sci. Reports* **1998**, *32*, 5.
11. Heffelfinger, J. R.; Bench, M. W.; Carter, C. B. *Surf. Sci.* **1997**, *370*, L168.
12. Causá, M.; Dovesi, R.; Pisani, C.; Roetti, C. *Surf. Sci.* **1989**, *215*, 259.
13. Puchin, V. E.; Gale, J. D.; Shluger, A. L.; Kotomin, E. A.; Günster, J.; Brause, M.; Kempfer, V. *Surf. Sci.* **1997**, *370*, 190.
14. Batyrev, I.G.; Alavi, A.; Finnis, M.W. *Faraday Discuss.* **1999**, *114*, 33.
15. Baxter, R.; Reinhardt, P.; López, N.; Illas, F. *Surf. Sci.* **2000**, *445*, 448.
16. Zhukovskii, Yu. F.; Alfredsson, M.; Hermansson, K.; Heifets, E.; Kotomin, E. A. *Nucl. Instr. Meth. Phys. Res. B* **1998**, *141*, 73.
17. Verdozzi, C.; Jennison, D. R.; Schultz, P. A.; Sears, M. P. *Phys. Rev. Letters* **1999**, *82*, 799.
18. Batyrev, I. G.; Alavi, A.; Finnis, M. W.; Deutsch, T. *Phys. Rev. Letters* **1999**, *82*, 1510.
19. Batyrev, I. G.; Kleinman, L. *Phys. Rev. B* **2001**, *64*, 033410.
20. Song, G.; Remhof, A.; Theis-Brohl, K.; Zabel, H. *Phys. Rev. Letters*, **1997**, *79*, 5062.
21. Saunders, V. R.; Dovesi, R.; Roetti, C.; Causà, M.; Harrison, N. M.; Orlando, R.; Zicovich-Wilson, C.M. *CRYSTAL98. User Manual*; Univ. Torino: Turin, 1999.
22. Perdew, J. P.; Wang, Y. *Phys. Rev. B* **1992**, *45*, 13244.
23. Catti, M.; Valerio, G.; Dovesi, R.; Causá, M. *Phys. Rev. B* **1994**, *49*, 14179.
24. Hay, P. J.; Wadt, W. R. J. *Chem. Phys.* **1985**, *82*, 284.
25. Wyckoff, R. W. G. *Crystal Structures* (2nd ed.); Wiley-Interscience: New York. V. 1, 1963.
26. Towler, M.D.; Zupan, A.; Causá M. *Comput. Phys. Commun.* **1996**, *98*, 181.
27. Zhukovskii, Yu. F.; Kotomin, E. A.; Jacobs, P. W. M.; Stoneham, A. M.; Harding, J. H. *Surf. Sci.* **1999**, *441*, 373.
28. Zhukovskii, Yu. F.; Kotomin, E. A.; Jacobs, P. W. M.; Stoneham, A. M. *Phys. Rev. Letters* **2000**, *84*, 1256.